



## NMR-BASED METABONOMICS STUDY OF SUB-ACUTE HEPATOTOXICITY INDUCED BY SILICA NANOPARTICLES IN RATS AFTER INTRANASAL EXPOSURE

A. PARVEEN<sup>1</sup>, S. H. M. RIZVI<sup>1</sup>, A. GUPTA<sup>2</sup>, R. SINGH<sup>1</sup>, I. AHMAD<sup>3</sup>, F. MAHDI<sup>4</sup> AND A. A. MAHDI<sup>1</sup>\*

<sup>1</sup> Department of Biochemistry, King George's Medical University, Lucknow, India

<sup>2</sup> Centre of Biomedical Magnetic Resonance, SGPGIMS Campus, Lucknow, India

<sup>3</sup> Fibre Toxicology Division, CSIR-Indian Institute of Toxicology Research, Lucknow, India

<sup>4</sup> Department of Biochemistry, Era's Lucknow Medical College & Hospital, Lucknow, India

### Abstract

Silica nanoparticles (SiO<sub>2</sub> NPs) are widely used commercially; however, their potential toxicity on human health has attracted particular attention. In the present study, the intranasal toxicological effect of 10nm and 80nm SiO<sub>2</sub> NPs (dosed at 150µg for 90 days) on rats was investigated using conventional approaches and metabonomics analysis of serum. Oxidative stress was measured by assessing Lipid peroxide (LPO) levels and enzymatic activities of Superoxide dismutase (SOD), Catalase (CAT), and Glutathione (GSH) levels in liver tissue homogenate. These biochemical observations were supplemented by histological examination of liver sections. SiO<sub>2</sub> NPs enhanced lipid peroxidation with concomitant reduction in SOD, CAT, and GSH content. In addition, SiO<sub>2</sub> NPs also produced alterations in hepatic histopathology. We also evaluated the effect of SiO<sub>2</sub> NPs on the activities of hepatic enzymes such as aminotransferases (ALT/AST) and alkaline phosphatase (ALP) which revealed significant increase in their activity when compared with control. Metabonomic profile of 90 days SiO<sub>2</sub> NPs treated rat sera exhibited significant increase in lactate, alanine, acetate, creatine and choline coupled with a considerable decrease in glucose level. These perturbations, on the whole, implicate impairment in tricarboxylic acid cycle and liver metabolism, which suggests that silica nanoparticles may have a potential to induce hepatotoxicity in rats.

**Key words:** Nanoparticles, Intranasal, Metabonomic, Hepatotoxicity.

### Article information

Received on May 16, 2012

Accepted on June 25, 2012

### \* Corresponding author

Tel: +91-9839011192

Fax: +91-522-2253030

E-mail: mahdiaa@rediffmail.com

### INTRODUCTION

The recent development of technology for reducing material size has provided innovative nanomaterials. While unique physicochemical properties of nanomaterials such as size, surface area, chemical composition, solubility, shape, aggregation state, etc., may enhance their biological reactivity, however, the properties that make nanomaterials attractive for commercial and medical use may also enhance their toxicity as materials that are inert in bulk form may be toxic in nano-size forms. It is thus essential to probe the potential toxicity imposed on human health, by nanomaterials (39, 30, 35, 12). To date, among the physicochemical properties of nanomaterials, particle size plays an important role in interactions with biological systems, gaining increasing attention from nanotoxicology researchers (13). Particle size can influence the interaction of nanomaterials with the biological components of cells through the effects of the surface area (37, 2, 15, 27). Moreover, size dependent distribution of nanoparticles in the body has been studied (8, 17, 5) which indicates that size is an important physicochemical property of nanomaterials which governs where and how the body react to the particles. For example, nanoparticles can easily enter tissues, and cross cell membranes, allowing them to harm the biological system (12, 10). But the correct matrix of relationship between particle size and biological response remains largely unclear, because some studies show that nano-sized particles cannot be generalized as always being more toxic than micro-sized particles (19).

Silica (SiO<sub>2</sub>) nanoparticles, are one of the most widely used nanomaterials developed for a broad spectrum of

biomedical and biotechnological applications (48, 18, 9, 38) such as biosensors for DNA (48), cancer therapy (18) gene delivery and drug delivery (9, 39, 4) etc. It has been reported that SiO<sub>2</sub> nanoparticles cause inflammatory responses (3, 6), hepatotoxicity (34, 24), neurotoxicity (7, 46) as well as fibrosis, and their tissue distribution and excretion differ depending on particle size (20). While on one hand Nishimori *et al.* reported increased serum markers of liver injury on administration of nanotized silica particles (34), Cho *et al.* demonstrated that submicron-sized silica particles with a diameter of 100 or 200 nm significantly increased the incidence and severity of liver inflammation, whereas the effects of nano-sized particles with a diameter of 50 nm were non-significant (5). One important thing is that these studies were based on intravenously administered silica particles, but the influence of inhalation of silica nanoparticles on hepatic system has not been investigated till date. While inhalation exposure to quartz, mineral dust particles and asbestos has been widely investigated to induce inflammation, fibrosis and cytotoxicity in the lung (35), the influence of inhalation exposure on hepatic system is not well documented. Knowing that inhaled nanoparticles do not locally remain in the lung but are also distributed to distant organs, such as the liver, kidney, brain and heart etc. through blood flow (20, 43, 31, 32), hence, the systemic effects of nanomaterials on various organs would be indispensable.

The present study was carried out to investigate the effect of intra-nasal exposure of silica nanoparticles on rat hepatic system. We have also applied NMR based metabonomics approach to investigate the metabolic profile of exposed rat serum, together with serum biochemistry, histo-

pathology examinations and antioxidant enzymes activity.

## MATERIALS AND METHODS

### *Silica nanoparticles and their characterization*

Two sizes, 10nm and 80nm, of silica nanoparticles ( $\text{SiO}_2$ ) were purchased from Nano Amor (Nanostructured & Amorphous Materials Inc., Houston, TX, USA, www.nanoamor.com). The detailed characteristics provided by the supplier are given in Table 1. These silica nanoparticles contained very little amount of trace metals. For example silica 10nm and silica 80nm contained iron <0.001% and 0.00002%, respectively. Furthermore, the size of  $\text{SiO}_2$  was confirmed using transmission electron microscopy (TEM) (figure 1).

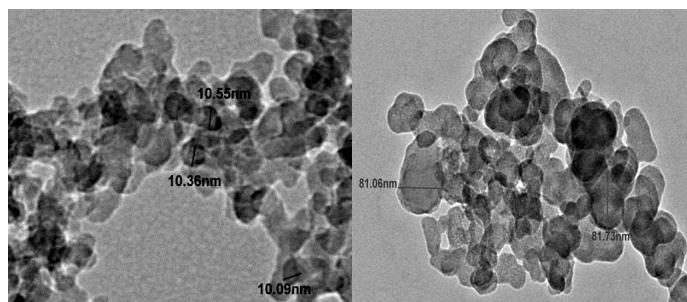


**Figure 1.** TEM image of the (a) 10nm (b) 80nm silica nanoparticles.

### *Animal handling and dosing*

18 young male Wistar rats (weight range,  $200 \pm 20$  g) were obtained from Indian Institute of Toxicology Research, Lucknow, India and were acclimatized. Rats were housed individually in metabolic cages in a well-ventilated room under controlled conditions (Temperature, humidity, and a 12-h light-dark Cycle). Food and tap water were provided ad libitum. All animal experiments were carried out in accordance with the guidelines established by the Association for Assessment and Accreditation of Laboratory Animal Care (AAALAC). After seven days of acclimatization, rats were randomly assigned into three groups with 6 rats in each group; group 1 was control group and while group 2 and 3 were experimental groups, treated with 10nm and 80nm  $\text{SiO}_2$  nanoparticles, respectively. We prepared  $\text{SiO}_2$  (10nm and 80nm) suspension using physiological saline solution at concentration of  $150 \mu\text{g}/50 \mu\text{l}$ , and  $50 \mu\text{l}$  of nanoparticles suspension intranasally instillation into both nostrils of rats for 90 days. Before instillation, nanoparticles suspension was sonicated to minimize the agglomeration. Control rats were treated with equivalent volume of physiological saline to minimize the time-dependent changes.

### *Sample collection*

Blood samples (2mL) were obtained by venipuncture aseptically after 90 days of treatment. Immediately after the collection, an aliquot of blood was placed in a sterile stoppered test tube and was allowed to coagulate for 30 min and centrifuged at 3000 rpm for 5min at  $4^\circ\text{C}$  to separate the sera. Serum samples were stored at  $-80^\circ\text{C}$  until analysed. Serum samples were used for clinical enzyme and serum metabolites analysis. Liver samples were collected and used for assessment of enzymatic activity and Histo-pathological analysis.

### *Histological analysis*

The liver tissue were removed and fixed with 4% para-formaldehyde. Thin sections of tissue were prepared using microtome which were then stained with hematoxylin and eosin for histological observation.

### *Clinical Enzymes*

Serum alkaline phosphatase (ALP), aspartate aminotransferases (AST) and alanine aminotransferases (ALT), were measured by an automated biochemical analyzer (Chemwell Biochemistry Autoanalyzer, USA).

### *Nuclear Magnetic Resonance Experiments*

$^1\text{H}$  NMR spectra for all serum were obtained on a 800 MHz spectrometer (Bruker, India Pvt Ltd) using 5-mm broad band inverse probe head at 300 K. Serum samples ( $500 \mu\text{L}$  each) were taken in 5-mm NMR tubes, a sealed coaxial capillary tube containing 0.375% trimethyl silyl propionic acid sodium salt- $d_4$  (TSP) in  $35 \mu\text{L}$  deuterium oxide and were inserted into the NMR tube before obtaining the NMR spectra. TSP served as a chemical shift reference as well as the standard signal for absolute quantitative estimation of the metabolites, whereas deuterium oxide served as solvent for “field-frequency locking.” One-dimensional  $^1\text{H}$  NMR spectra were obtained for the samples using one-pulse sequence with suppression of water resonance by presaturation. For all the serum samples, additional one-dimensional  $^1\text{H}$  NMR spectra were also obtained using Carr–Purcell–Meiboom–Gill (CPMG) pulse sequence with suppression of water resonance by presaturation to remove the broad resonances arising from macromolecules. The typical parameters used were spectral width: 8000 Hz; time domain points: 32K; relaxation delay: 5 s; pulse angle:  $90^\circ$ ; number of scans: 64; spectrum size: 32 K and line broadening: 0.3 Hz. For CPMG experiment total echo time of 0.64 ms with 420 echoes was used. The concentrations of metabolites were obtained using the

**Table 1.** Representing average particle size and specific surface area (Data provided by manufacturer).

Nanoparticle products IDs	Nanoparticle size	Chemical formulae	Purity(%)	SSAb (m <sup>2</sup> /g)	Color	Morphology
4850MR	10nm(ASP)2	SiO <sub>2</sub> , amorphous	99.5	640	White	Spherical, porous
4830 HT	80nm(APS)	SiO <sub>2</sub> , amorphous	99.0	440	White	Spherical

Data provided by manufacturer. Note: The purity of nanoparticles.

<sup>2</sup> Average particle size

<sup>b</sup> Specific surface area measured by BET (Brunauer-Emmett-Edward)

integral area of respective metabolite marker signal with reference to the integral area of TSP in CPMG spectra (45).

### Biochemical analysis

#### Homogenate preparation

After 90 days of SiO<sub>2</sub> nanoparticles administration rats were sacrificed; their liver were removed and weighed individually for biochemical analysis. Ten percent (w/v) homogenate of the liver tissue was prepared by of York's homogenizer fitted with Teflon plunger in 0.1 M phosphate buffer (pH 7.1). The whole homogenate was first centrifuged at 2500 ×g for 10 min in a refrigerated centrifuge. The pellet consisting of nuclear fraction and cell debris was discarded. The supernatant was further centrifuged at 11,000 ×g for 15 min and mitochondrial fraction was separated. The clear supernatant was further centrifuged at 105,000 ×g for 90 min and the resultant supernatant was used for determining enzyme activities.

#### Measurement of protein oxidation and lipid peroxidation

The protein content was measured by the method of Lowry *et al.* (26) using bovine serum albumin (BSA) as standard. The lipid peroxide (LPx) levels were measured by the method of Ohkawa *et al.* (36). The thiobarbituric acid reacting substances (TBARS) of the sample were estimated spectrophotometrically at 532nm and expressed as nmol of MDA/ g tissue .

#### Measurement of superoxide dismutase activity

An aliquot of liver homogenate was used for the assay of enzymatic antioxidants. The superoxide dismutase (SOD EC 1: 15.1.1) activity was determined from its ability to inhibit the reduction of NBT in presence of PMS according to the method of McCord and Fridovich (29). The reaction was monitored spectrophotometrically at 560 nm. The SOD activity was expressed as U/mg protein (1 U is the amount of enzyme that inhibit the reduction of NBT by

one half in above reaction mixture) .

#### Measurement of catalase activity

Catalase (CAT, EC 1.11.1.6) activity was assayed as per the method of Aebi (1) using hydrogen peroxide as substrate; the decomposition of H<sub>2</sub>O<sub>2</sub> was followed at 240 nm on spectrophotometer. The CAT activity was expressed as U/mg protein.

#### Measurement of reduced glutathione

The Reduced glutathione was measured in deprotonized supernatant from liver homogenate. Tissue homogenate was deproteinated with tetrachloroacetic acid, centrifuged and supernatant was used for the estimation of reduced glutathione (GSH) by the use of Ellman reagent (5, 5'-dithiobis (2- nitro benzoic acid). The optical density of the pale colour was measured on the spectrophotometer on 412 nm. An appropriate standard (pure GSH) was run simultaneously. The level of GSH was expressed as µg/g tissue (11).

#### Statistical Analysis

Statistical analysis was carried out by one way analysis of variance (ANOVA) involving Newman-Keuls test for posthoc comparisons. The level of significance was accepted at p<0.05.

## RESULTS

#### Effect of SiO<sub>2</sub> nanoparticles on liver histology

The liver of control rats showed normal histological structure, whereas silica nanoparticles treated rats showed degenerative changes as evident in numerous hepatocytes (Figur-2), the cells were enlarged, and had light and foamy cytoplasm filled with vacuoles.

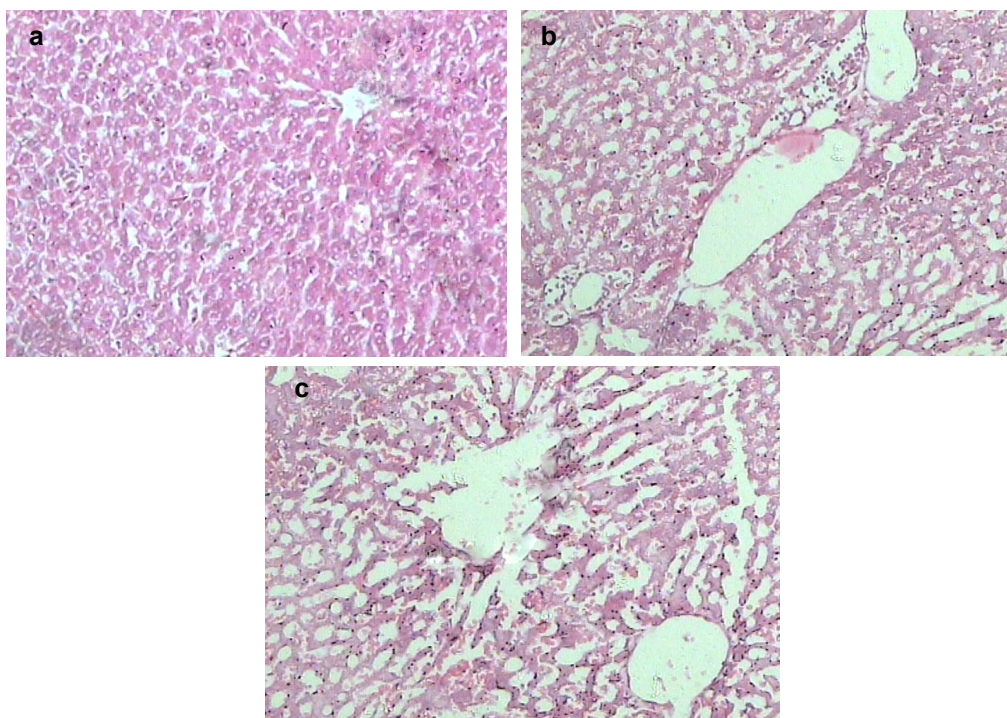


**Figure 2.** Representing Light photomicrograph of (H&E) staining (a) Control rat liver tissue showing normal architecture of central vein, sinusoids, and hepatocytes [40×], (b) and (c) 10nm and 80nm silica nanoparticles treated rat, liver tissue for 90 days showing the trabecular structure of the lobules blurred in places. The cytoplasm of some hepatocytes is enlarged and vacuolated. (40×).

### Effect of SiO<sub>2</sub> nanoparticles on Clinical Enzymes

The blood biochemical parameters that reflect the hepatic functions were further investigated. Serum AST and ALP levels were significantly increased in both 10nm and 80nm silica nanoparticles treated groups with respect to control groups. While serum ALT level was significantly increased only in rats treated with 10nm silica nanoparticles, no significant changes were observed in ALT levels in 80nm silica nanoparticles treated groups (Figure-4).

### <sup>1</sup>H NMR spectroscopic measurement of serum

Typical <sup>1</sup>H NMR serum spectra of 90 days of 10nm SiO<sub>2</sub> and 80nm SiO<sub>2</sub> treated rats and that of controls are shown in Figure 3. Twelve metabolites, viz. lactate, alanine, acetate, glutamate, pyruvate, glutamine, creatine, choline, threonine, glucose, histidine, and formate were identified and quantified using their respective <sup>1</sup>H NMR signals. The concentrations of these twelve serum metabolites for 90 days of 10nm SiO<sub>2</sub> and 80nm SiO<sub>2</sub> treated rats and that of control rats are shown in Table 2 along with statistical evaluation. A significant increase in lactate, alanine, acetate, creatine, choline, were observed in 90-days 10nm SiO<sub>2</sub> and 80nm SiO<sub>2</sub> treated rats, whereas a significant decrease in glucose levels was observed in 90 days of 10nm SiO<sub>2</sub> and 80nm SiO<sub>2</sub> treated rats compared with controls. Other metabolites were statistically remains unaltered (Table-2 and figure 3).

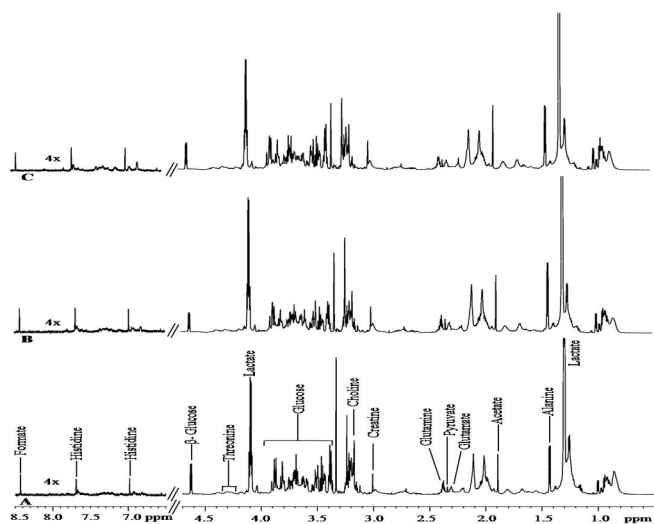


**Figure 3.** <sup>1</sup>H NMR spectra of serum of (A) control rats (B) and (C) 10nm SiO<sub>2</sub> and 80nm SiO<sub>2</sub> treated rats.

**Table 2.** Serum metabolites of the rats exposed to the 10nm and 80nm SiO<sub>2</sub>. Value are mean ± SD of six animals in each group. The asterisk indicates the significant difference between 10nm and 80nm SiO<sub>2</sub> groups compared to control group \*significantly differs (p < 0.05).

	Lactate	Alanine	Acetate	Glutamate	Pyruvate	Glutamine
<b>Control</b>	646.9 ± 40.7	89.58 ± 12.7	21.65 ± 7.5	79.32 ± 10.2	10.32 ± 2.7	118.3 ± 19.1
<b>10nm SiO<sub>2</sub></b>	792.4 ± 87.6*	115.4 ± 24.4*	30.41 ± 3.8*	89.25 ± 11.5	10.06 ± 2.1	109.6 ± 10.1
<b>80nm SiO<sub>2</sub></b>	800.1 ± 52.3*	113.1 ± 20.4*	30.58 ± 5.0*	86.16 ± 9.2	11.36 ± 2.3	115.3 ± 24.6
	Creatine	Choline	Threonine	Glucose	Histidine	Formate
<b>Control</b>	29.39 ± 6.0	8.58 ± 1.5	81.93 ± 20.5	379.32 ± 30.2	9.32 ± 2.5	0.51 ± 0.1
<b>10nm SiO<sub>2</sub></b>	35.75 ± 5.1*	24.06 ± 3.2*	73.22 ± 20.4	206.5 ± 23.5*	11.16 ± 2.6	0.55 ± 0.2
<b>80nm SiO<sub>2</sub></b>	36.65 ± 3.4*	25.83 ± 3.0*	76.58 ± 15.0	226.3 ± 26.2*	11.26 ± 2.4	1.13 ± 0.3

### Effect of SiO<sub>2</sub> nanoparticles on total protein content

The total protein content was found to be decreased in both 10nm and 80nm silica nanoparticles exposed groups with respect to the controls, but no significant changes were observed between groups, however, the magnitude of reduction was slightly higher in 10nm silica nanoparticles exposed group (Figure 5).

### Effect of SiO<sub>2</sub> nanoparticles on lipid peroxidation

The level of malonaldehyde (MDA) was significantly increased in 10nm and 80nm silica nanoparticles exposed groups with respect to controls in liver tissue, but characteristically the magnitude of lipid oxidation was slightly less in 80nm silica nanoparticles treated group than 10nm Silica nanoparticles exposed rats, and no significant changes were observed in between both treated groups (Figure 5).

### Effect of SiO<sub>2</sub> nanoparticles on SOD and CAT activity

The activity of superoxide dismutase (SOD) and Catalase (CAT) were significantly decreased in 10nm and 80nm silica nanoparticles treated groups when compared with controls, while no significant changes were observed between the groups (Figure 5).

### Effect of SiO<sub>2</sub> nanoparticles on reduces glutathione content

A significant decrease in reduced glutathione (GSH) levels in liver tissue was observed in rats following exposure to 10nm and 80nm SiO<sub>2</sub> nanoparticles when compared to controls (Figure 5).

## DISCUSSION

Silica nanoparticles are emerging as a new and promising class of nanoparticles that have been developed for drug delivery system due to their special structure and functions (22, 23). Therefore, concerns on the biosafety impact of silica nanoparticles are being increasingly discussed (16, 41, 42, 44). Previous studies reported that inhalation of SiO<sub>2</sub> nanoparticles causes pulmonary inflammation, cardiovascular alterations and neurotoxicity in rats, however, the influence of inhalation exposure of silica nanoparticles on hepatic system is not well documented. As we know that inhaled nanoparticles can enter the blood and from systemic circulation reach to distant organs, such as the liver,

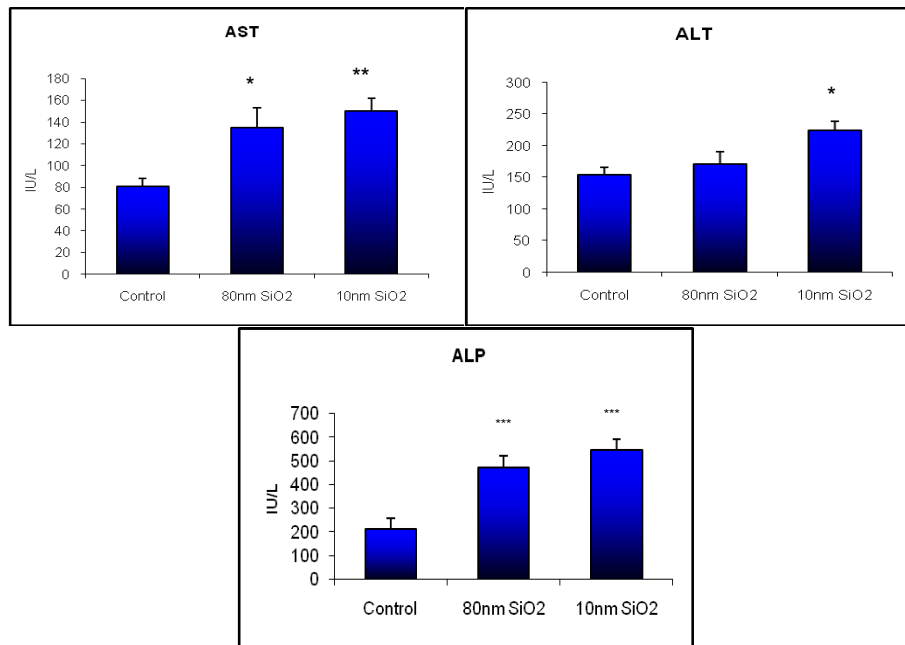


**Figure 4.** Clinical chemistry indexes of rats following intranasal exposure of silica Nanoparticles, AST, ALT and ALP level in serum of the rats exposed to the 10nm and 80nm SiO<sub>2</sub>. Values are mean ± SD of six animals in each group. The asterisk indicates the significant difference between 10nm and 80nm SiO<sub>2</sub> groups compared to control group (\*p < 0.05), (\*\*p < 0.01), (\*\*p < 0.001).

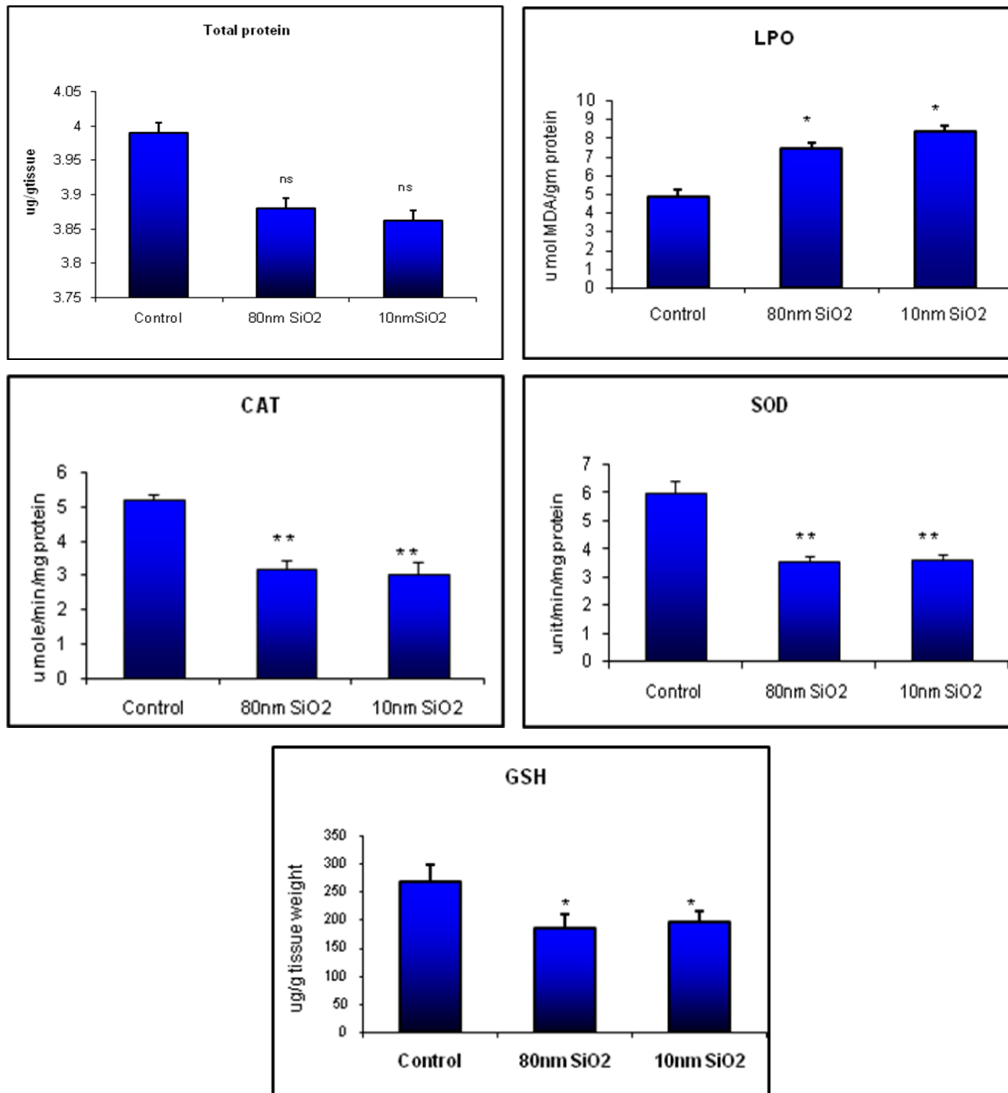


**Figure 5.** LPO, CAT, SOD and GSH level in liver tissue of the rats exposed to the 10nm and 80nm SiO<sub>2</sub>. Value are mean ± SD of six animals in each group. The asterisk indicates the significant difference between 10nm and 80nm SiO<sub>2</sub> groups compared to control group (\*p < 0.05) (\*\*p < 0.01) and na indicates non significant.

kidney, brain and heart (20, 43, 31, 32). Thus, it is necessary to confirm the influence of nanomaterials in systemic flow on various organs. In the present study, we evaluated the sub-acute hepatotoxicity induced by intranasal exposure of silica (10nm and 80nm) nanoparticles and found that rats treated with 150 $\mu$ g silica nanoparticles intranasally for 90 days exhibited evidence of hepatotoxicity. Several hepatotoxicity studies have suggested that liver may be the major target organ for the nanomaterials (34, 25) and these nanoscale materials may be toxic when they enter the blood stream directly or indirectly. Our observations from the pathological examinations showed degenerative necrosis in hepatocytes and enlarged cells with light and foamy vacuolar cytoplasm in both 10nm and 80nm SiO<sub>2</sub> nanoparticles treated rats, which clearly indicate liver injury. Moreover, the blood biochemical parameters reflected loss of hepatic functions with the significant elevation in the level of ALP and AST enzyme activity. These findings are consistent with the previous reports illustrating liver injury and altered serum biomarkers induced by 70nm silica nanoparticles administered at a dose of 30 mg/kg body weight (34). Furthermore, our results on SiO<sub>2</sub> nanoparticles by intranasal instillation were similar to those with intravenous instillation.

An elevated level of lactate, alanine, acetate, creatine and choline (with 90-days SiO<sub>2</sub> treatment) as evident from NMR studies, in serum is indicative of hepatic dysfunction, which indicates perturbation in glycolytic and tricarboxylic acid cycle pathways of hepatocytes. Possibly, SiO<sub>2</sub> causes ischemic injury of hepatocytes which impairs the enzymatic activity related to the metabolism of glucose and amino acids and hence the liver cells are unable to effectively metabolize carbohydrates and proteins, resulting in an increase in lactate, alanine and acetate in the serum. The increase in blood creatine could be related to the dysfunction of glomerular filtrate while lower rates of glomerular filtration or lack of reabsorption of creatine in the glomerulus is expected due to perturbation of the rennin-angiotensin system (33). A higher concentration of choline indicates degradation of cell membrane, liver cell death, or liver cell proliferation. Excess choline indicates that there is loss of mobilization of fat from liver (lipotropic action) due to inflammation of hepatocytes caused by hyper-activation of platelet-activating factor and other cellular dysfunctions (14). The reduction in glucose levels indicate mitochondrial dysfunction, which possibly leads to alternative metabolic pathway especially in rat models, resulting in perturbation of glycolysis and TCA cycle (27). Significantly lower concentration of glucose levels in SiO<sub>2</sub> nanoparticles-treated rat is another indication of liver damage.

Hepatocytes derive most of their energy from glucose; hence, impaired glycolysis, TCA cycle and electron transport chain, as observed in SiO<sub>2</sub> nanoparticles toxicity (28), may lead to decreased ATP production and increased formation of free radicals resulting in oxidation of mitochondrial DNA, proteins and lipids (47). Moreover, our results also showed high level of lipid peroxides in the liver of nanoparticles treated rats, indicating involvement of severe oxidative stress which is closely related to the reduction in activities of antioxidant enzymes like SOD and CAT as well as depletion of non-enzymatic antioxidants like GSH. Till date, the mechanism for the generation of oxidative stress after nanoparticles treatment is still

not clear, but Singh *et al.* (40) suggested that it is related to the large particle surface area. Cellular oxidative stress following exposure with different sized SiO<sub>2</sub> (10nm and 80nm) nanoparticles remained almost same and no obvious evidence of greater toxicity being associated with large surface area could be observed. Li *et al.* (21) compared pulmonary toxicity of 3nm and 20nm TiO<sub>2</sub> nanoparticles *in vivo* and reported similar results. The size effect of nanoparticles in toxicity needs to be further explored.

To conclude it may be stated that the abnormal metabolic profiles of rat serum, as evident from 1H NMR spectroscopic analysis, reflect the altered cellular metabolic pathway mechanism caused by SiO<sub>2</sub> nanoparticles and this is directly coupled to the perturbed blood biochemistry. These metabolic changes can be exploited as the symptoms of SiO<sub>2</sub> nanoparticles toxicity in the rat liver and serum. However, further evaluation of the relationship between toxicity, size, shape and chemical modification of the surface of particles is needed, and the future studies based on these data may provide very useful information for development of drug delivery system and other aspects of using nano-size materials.

#### ACKNOWLEDGEMENTS

The authors thank Prashant Singh Shakya for his assistance in preparing sample, NMR data acquisition and analysis. Financial support was provided by Council of Science & Technology U. P.

Other articles in this theme issue include references (49-76).

#### REFERENCES

1. Aebi, H., In: *Methods of Enzymatic Analysis Vol. 2*, Bergmeyer HU (ed.), Academic Press Inc. New York, 1974, pp. 673-684.
2. Brown, D.M., Wilson, M.R., MacNee, W., Stone, V. and Donaldson, K., Size-dependent proinflammatory effects of ultrafine polystyrene particles: a role for surface area and oxidative stress in the enhanced activity of ultrafines. *Toxicol. Appl. Pharmacol.* 2001, **175**: 191-199.
3. Cao, Q., Zhang, S., Dong, C. and Song, W., Pulmonary responses to fine particles: differences between the spontaneously hypertensive rats and wistar kyoto rats. *Toxicol. Lett.* 2007, **171**: 126-37.
4. Chen, J. F., Ding, H. M., Wang, J. X., Shao, L., Preparation and characterization of porous hollow silica nanoparticles for drug delivery application. *Biomaterials.* 2004, **25**: 723-727.
5. Cho, M., Cho, W.S., Choi, M., Kim, S.J., Han, B.S., Kim, S.H., Kim, H.O., Sheen, Y.Y. and Jeong, J., The impact of size on tissue distribution and elimination by single intravenous injection of silica nanoparticles, *Toxicol. Lett.* 2009, **189**: 177-83.
6. Cho, W. S., Choi, M., Han, B.S., Cho, M., Oh, J., Park, K., Kim, S.J., Kim, S.H. and Jeong, J., Inflammatory mediators induced by intratracheal instillation of ultrafine amorphous silica particles. *Toxicol. Lett.* 2007, **175**: 24-33.
7. Choi, J., Zheng, O., Katz, H.E., Silica-Based Nanoparticle Uptake and Cellular Response by Primary Microglia. *Environmental Health Perspectives* . 2010, **118**: 589-595.
8. De Jong, W. H., Hagens, W. I., Krystek, P., Burger, M. C., Sips, A. J. and Geertsma, R.E., Particle size-dependent organ distribution of gold nanoparticles after intravenous administration. *Biomaterials.* 2008, **29**: 1912-1919.
9. Dhruva, J., Klejbor, B.I., Stachowiak, E.K., Dutta, P., Roy, I., Kaur, N., Bergey, E.J., Prasad, P.R. and Stachowia, M.K., Organically modified silica nanoparticles: A nonviral vector for *in vivo* gene delivery and expression in the brain. *PNAS.* 2005, **102**: 11539-11544.
10. Donaldson, K., Stone, V., Tran, C.L., Kreyling, W. and Borm, P.J.,

Nanotoxicology. *Occup Environ Med.* 2004, **9**: 727-728.

11. Ellman, G.L., Tissue sulfhydryl groups. *Arch Biochem Biophys.* 1959, **82**: 70.

12. Fischer, H.C., and Chan, W. C., Nanotoxicity: the growing need for *in vivo* study *Curr. Opin. Biotechnol.* 2007, **18**: 565-71.

13. Foster, K. A., Yazdaniyan, M., Audus, K.L., Microparticulate uptake mechanisms of *in vitro* cell culture models of the respiratory epithelium. *J. Pharm. Pharmacol.* 2001, **53**: 57-66.

14. Griffin, J.L., Mann, C.J., Scott, J., Shoulders, C.C. and Nicholson, J. K., Choline containing metabolites during cell transfection: an insight into magnetic resonance spectroscopy detectable changes. *FEBS Lett.* 2001, **509**: 263-6.

15. Hagens, W. I., Oomen, A. G., de Jong, W. H., Cassee, F. R. and Sips, A. J., What do we (need to) know about the kinetic properties of nanoparticles in the body? *Regul. Toxicol. Pharmacol.* 2007, **49**: 217-29.

16. Hamilton, Jr.R.F., Thakur, S.A., Mayfair, J.K, Holian, A., MARCO mediates silica uptake and toxicity in alveolar macrophages from C57BL/6 mice. *J Biol Chem.* 2006, **281**: 34218-26.

17. Hillyer, J.F. and Albrecht, R.M., Gastrointestinal persorption and tissue distribution of differently sized colloidal gold nanoparticles. *J. Pharm. Sci.* 2001, **90**: 1927-36.

18. Hirsch, L. R., Stafford, R. J., Bankson, J. A., Sershen, S. R., Rivera, B., Price. Nanoshell-mediated near-infrared thermal therapy of tumors under magnetic resonance guidance. *Proc. Natl. Acad. Sci. U. S. A.* 2003, **100**: 13549-13554.

19. Karlsson, H.L., Gustafsson, J., Cronholm, P. and Moller, L., Size-dependent toxicity of metal oxide particles - a comparison between nano- and micrometer size. *Toxicol. Lett.* 2009, **188**: 112-118.

20. Kim, J.S., Yoon, T.J., Yu, K.N., Kim, B.G., Park, S.J., Kim, H.W., Lee, K.H., Park, S.B., Lee, J.K., Cho, M.H., Toxicity and tissue distribution of magnetic nanoparticles in mice. *Toxicol. Sci.* 2006, **89**: 338-347.

21. Li, J., Li, Q., Xu, Q., Li, J., Cai, X., Liu, R., Li, Y., Ma, J., Li, W., Comparative study on the acute pulmonary toxicity induced by 3 and 20nm TiO<sub>2</sub> primary particles in mice. *Environ. Toxicol. Pharmacol.* 2007, **24**: 239-244.

22. Li, L., Tang, F., Liu, H., Liu, T., Hao, N., Chen, D., In vivo delivery of silica nanorattle encapsulated docetaxel for liver cancer therapy with low toxicity and high efficacy. *AcsNano* 2010, **4**: 6874-82.

23. Liu, H., Chen, D., Li, L., Liu, T., Tan, L., Wu, X., Multifunctional gold nanoshells on silica nanorattles: a platform for the combination of photothermal therapy and chemotherapy with low systemic toxicity. *Angew Chem Int Ed Engl.* 2011, **50**: 891-895.

24. Liu, T., Li, L., Fu, C., Liu, H., Chen, D., Tang, F., Pathological mechanisms of liver injury caused by continuous intraperitoneal injection of silica nanoparticles. *Biomaterials.* 2012, **33**: 2399-2407.

25. Liu, T., Li, L., Teng, X., Huang, X., Liu, H., Chen, D., Single and repeated dose toxicity of mesoporous hollow silica nanoparticles in intravenously exposed mice. *Biomaterials.* 2011, **32**: 1657-1668.

26. Lowry, O.H., Rosebrough, N.J., Farr, A.L., Randall, R.J., Protein measurement with the Folin phenol reagent. *J. Biol. Chem.* 1951, **193**: 265-268.

27. Lu, X., Tian, Y., Zhao, Q., Jin, T., Xiao, S. and Fan, X., Integrated metabonomics analysis of the size-response relationship of silica nanoparticles-induced toxicity in mice. *Nanotechnology.* 2011, **22**: 16-21.

28. Lu, X., Tian, Y., Zhao, Q., Jin, T., Xiao, S. and Fan, X., Integrated metabonomics analysis of the size-response relationship of silica nanoparticles-induced toxicity in mice. *Nanotechnology.* 2011, **22**: 16-22.

29. McCord, J.M., Fridovich, I., SOD enzyme function for erythrocyte. *J. Biol. Chem.* 1969, **224**: 6049-6055.

30. Nel, A., Xia, T., Madler, L., Li, N., Toxic potential of materials at

the nano level. *Science.* 2006, **311**: 622-627.

31. Nemmar, A., Hoet, P.H., Vanquickenborne, B., Dinsdale, D., Thomeer, M., Hoylaerts, M.F., Vanbilloen, H., Mortelmans, L., Nemery, B., Passage of inhaled particles into the blood circulation in humans. *Circulation.* 2002, **105**: 411-414.

32. Nemmar, A., Vanbilloen, H., Hoylaerts, M.F., Hoet, P.H., Verbruggen, A., Nemery, B., Passage of intratracheally instilled ultrafine particles from the lung into the systemic circulation in hamster. *Am. J. Respir. Crit. Care Med.* 2001, **164**: 1665-1668.

33. Nicholson, J.K., Timbrell, J.A., Sadler, P.J., Proton NMR spectra of urine as indicators of renal damage. Mercury induced nephrotoxicity in rats. *Mol Pharmacol.* 1985, **27**: 644-651.

34. Nishimori, H., Kondoh, M., Isoda, K., Tsunoda, S., Tsutsumi, Y. and Yagi, K., Silica nanoparticles as hepatotoxicants. *Eur. J. Pharm. Biopharm.* 2009, **72**: 496-501.

35. Oberdorster, G., Oberdorster, E., Oberdorster, J., Nanotoxicology: an emerging discipline evolving from studies of ultrafine particles. *Environ. Health Perspect.* 2005, **113**: 823-839.

36. Ohkawa, H., Ohishi, N., Yagi, K., Assay for lipid peroxides in animal tissue by thio-barbituric acid reaction. *Anal. Biochem.* 1979, **95**: 351-358.

37. Powers, K.W., Brown, S.C., Krishna, V. B., Wasdo, S.C., Moudgil, B.M. and Roberts, S.M., Research strategies for safety evaluation of nanomaterials. Part VI. Characterization of nanoscale particles for toxicological evaluation. *Toxicol. Sci.* 2006, **90**: 296-303.

38. Roy, I., Ohulchanskyy, T. Y., Bharali, D. J., Pudavar, H. E., Mistretta, R. A., Kaur, N., Prasad, P. N., Optical tracking of organically modified silica nanoparticles as DNA carriers: a nonviral, nanomedicine approach for gene delivery. *Proc. Natl. Acad. Sci. U. S. A.* 2005, **102**: 279-284.

39. Service, R.F., U.S. nanotechnology. Health and safety research slated for sizable gains. *Science* 2007; **315**: 926.

40. Singh, S., Shi, T., Duffin, R., Albrecht, C., van Berlo, D., Höhr, D., Fubini, B., Martra, G., Fenoglio, I., Borm, P.J., Schins, R.P., Endocytosis, oxidative stress and IL-8 expression in human lung epithelial cells upon treatment with fine and ultrafine TiO<sub>2</sub>: role of the specific surface area and of surface methylation of the particles. *Toxicol Appl Pharmacol.* 2007, **222**: 141-151.

41. Slowing, I.I., Vivero-Escoto, J.L., Wu, C.W., Lin, V.S., Mesoporous silica nanoparticles as controlled release drug delivery and gene transfection carriers. *Adv Drug Deliv Rev.* 2008, **60**: 1278-1288.

42. Slowing, I.I., Wu, C.W., Vivero-Escoto, J.L., Lin, V.S., Mesoporous silica nanoparticles for reducing hemolytic activity towards mammalian red blood cells. *Small.* 2009, **5**: 57-62.

43. Takenaka, S., Karg, E., Roth, C., Schulz, H., Ziesenis, A., Heinzmann, U., Schramel, P., Heyder, J., Pulmonary and systemic distribution of inhaled ultrafine silver particles in rats. *Environ. Health Perspect.* 2001, **109**: 547-551.

44. Tao, Z., Morrow, M.P., Asefa, T., Sharma, K.K., Duncan, C., Anan, A., Mesoporous silica nanoparticles inhibit cellular respiration. *Nano Lett.* 2008, **8**: 1517-26.

45. Tripathi, S., Somashekar, B.S., Mahdi, A.A., Gupta, A., Mahdi, F., Hasan, M., Roy, R., Khetrpal, C.L., Aluminum mediated metabolic changes in rat serum and urine: A proton NMR study. *Biochem Mol Toxicol.* 2008, **22**: 119-127.

46. Wu, J., Wang, C., Sun, J., Xue, Y., Neurotoxicity of Silica Nanoparticles: Brain Localization and Dopaminergic Neurons Damage Pathways. *ACS Nano.* 2011, **5**: 4476-4489.

47. Xia, T., Kovoichich, M. and Nel, A.E., Impairment of mitochondrial function by particulate matter (PM) and their toxic components: implications for PM-induced cardiovascular and lung disease. *Front. Biosci.* 2007, **12**: 1238-46.

48. Zhao, X. J., Tapeç-Dytioco, R., Tan, W. H., Nucleic Acid Conjugated Nanomaterials for Enhanced Molecular Recognition. *J. Am. Chem.*

*Soc.* 2003, **125**: 11474-11475.

49. Singh, M. P., and Kumar, V., Biodegradation of vegetable and agrowastes by *Pleurotus sapidus*: A noble strategy to produce mushroom with enhanced yield and nutrition. *Cell. Mol. Biol.* 2012, **58** (1): 1-7.
50. Pandey, V. K., Singh, M.P., Srivastava, A. K., Vishwakarma S. K., and Takshak, S., Biodegradation of sugarcane bagasse by white rot fungus *Pleurotus citrinopileatus*. *Cell. Mol. Biol.* 2012, **58** (1): 8-14.
51. Ruhail, A., Rana, J. S., Kumar S., and Kumar, A., Immobilization of malate dehydrogenase on carbon nanotubes for development of malate biosensor. *Cell. Mol. Biol.* 2012, **58** (1): 15-20.
52. Vishwakarma, S. K., Singh, M. P., Srivastava A.K. and Pandey, V. K., Azo dye (direct blue) decolorization by immobilized extracellular enzymes of *Pleurotus* species. *Cell. Mol. Biol.* 2012, **58** (1): 21-25.
53. Dash, S. K., Sharma, M., Khare, S. and Kumar, A., *rmpM* gene as a genetic marker for human bacterial meningitis. *Cell. Mol. Biol.* 2012, **58** (1): 26-30.
54. Bertolotti, F., Crespan, E. and Maga, G., Tyrosine kinases as essential cellular cofactors and potential therapeutic targets for human immunodeficiency virus infection. *Cell. Mol. Biol.* 2012, **58** (1): 31-43.
55. Sandalli, C., Singh, K., and Modak, M. J., Characterization of catalytic carboxylate triad in non-replicative DNA polymerase III (pol E) of *Geobacillus kaustophilus* HTA. *Cell. Mol. Biol.* 2012, **58** (1): 44-49.
56. Kaushal, A., Kumar, D., Khare, S. and Kumar, A., *speB* gene as a specific genetic marker for early detection of rheumatic heart disease in human. *Cell. Mol. Biol.* 2012, **58** (1): 50-54.
57. Datta, J. and Lal, N., Application of molecular markers for genetic discrimination of *Fusarium* wilt pathogen races affecting chickpea and pigeonpea in major regions of India. *Cell. Mol. Biol.* 2012, **58** (1): 55-65.
58. Siddiqi, N. J., Alhomida, A. S., Khan, A. H. and Onga, W.Y., Study on the distribution of different carnitine fractions in various tissues of bovine eye. *Cell. Mol. Biol.* 2012, **58** (1): 66-70.
59. Ong, Y. T., Kirby, K. A., Hachiya, A., Chiang, L. A., Marchand, B., Yoshimura, K., Murakami, T., Singh, K., Matsushita, S. and Sarafianos, S. G., Preparation of biologically active single-chain variable antibody fragments that target the HIV-1 GP120 v3 loop. *Cell. Mol. Biol.* 2012, **58** (1): 71-79.
60. Singh, J., Gautam, S. and Bhushan Pant, A., Effect of UV-B radiation on UV absorbing compounds and pigments of moss and lichen of Schirmacher Oasis region, East Antarctica. *Cell. Mol. Biol.* 2012, **58** (1): 80-84.
61. Singh, V. P., Srivastava, P. K., and Prasad, S. M., Impact of low and high UV-B radiation on the rates of growth and nitrogen metabolism in two cyanobacterial strains under copper toxicity. *Cell. Mol. Biol.* 2012, **58** (1): 85-95.
62. Datta, J. and Lal, N., Temporal and spatial changes in phenolic compounds in response *Fusarium* wilt in chickpea and pigeonpea. *Cell. Mol. Biol.* 2012, **58** (1): 96-102.
63. Sharma, R. K., JAISWAL, S. K., Siddiqi, N. J., and Sharma, B., Effect of carbofuran on some biochemical indices of human erythrocytes *in vitro*. *Cell. Mol. Biol.* 2012, **58** (1): 103-109.
64. Singh, A. K., Singh, S. and Singh, M. P., Bioethics A new frontier of biological Science. *Cell. Mol. Biol.* 2012, **58** (1): 110-114.
65. Adedjei, A. O., Singh, K. and Sarafianos, S. G., Structural and biochemical basis for the difference in the helicase activity of two different constructs of SARS-CoV helicase. *Cell. Mol. Biol.* 2012, **58** (1): 115-121.
66. Singh, S., Choudhuri, G., Kumar, R. and Agarwal, S., Association of 5, 10-methylenetetrahydrofolate reductase C677T polymorphism in susceptibility to tropical chronic pancreatitis in North Indian population. *Cell. Mol. Biol.* 2012, **58** (1): 122-127.
67. Sharma, R. K., Rai, K. D. and Sharma, B., *In vitro* carbofuran induced micronucleus formation in human blood lymphocytes. *Cell. Mol. Biol.* 2012, **58** (1): 128-133.
68. Naraian, R., Ram, S., Kaistha S. D. and Srivastava J., Occurrence of plasmid linked multiple drug resistance in bacterial isolates of tannery effluent. *Cell. Mol. Biol.* 2012, **58** (1): 134-141.
69. Pandey, A. K., Mishra, A. K., And Mishra, A., Antifungal and antioxidative potential of oil and extracts, respectively derived from leaves of Indian spice plant *Cinnamomum tamala*. *Cell. Mol. Biol.* 2012, **58** (1): 142-147.
70. Mishra, N., and Rizvi, S. I., Quercetin modulates Na<sup>+</sup>/K<sup>+</sup> ATPase and sodium hydrogen exchanger in type 2 diabetic erythrocytes. *Cell. Mol. Biol.* 2012, **58** (1): 148-152.
71. Kumar, A., Sharma, B. and Pandey, R. S., Assessment of stress in effect to pyrethroid insecticides,  $\lambda$ -cyhalothrin and cypermethrin in a freshwater fish, *Channa punctatus* (Bloch). *Cell. Mol. Biol.* 2012, **58** (1): 153-159.
72. Srivastava N., Sharma, R. K., Singh, N. and Sharma, B., Acetylcholinesterase from human erythrocytes membrane: a screen for evaluating the activity of some traditional plant extracts. *Cell. Mol. Biol.* 2012, **58** (1): 160-169.
73. Singh, M.P., Pandey, A. K., Vishwakarma S. K., Srivastava, A. K. and Pandey, V. K., Extracellular Xylanase Production by *Pleurotus* species on Lignocellulosic Wastes under *in vivo* Condition using Novel Pretreatment. *Cell. Mol. Biol.* 2012, **58** (1): 170-173.
74. Kumar, S., Sharma, U. K., Sharma, A. K., Pandey, A. K., Protective efficacy of *Solanum xanthocarpum* root extracts against free radical damage: phytochemical analysis and antioxidant effect. *Cell. Mol. Biol.* 2012, **58** (1): 174-181.
75. Shukla, A., Singh, A., Singh, A., Pathak, L.P., Shrivastava, N., Tripathi, P. K., Singh, K. and Singh, M.P., Inhibition of *P. falciparum* PfATP6 by curcumin and its derivatives: A bioinformatic Study. *Cell. Mol. Biol.* 2012, **58** (1): 182-186.
76. Michailidis, E., Singh, K., Ryan, E. M., Hachiya, A., Ong, Y. T., Kirby, K. A., Marchand, B., Kodama, E. N., Mitsuya, H., Parniak, M.A. and Sarafianos, S.G., Effect of translocation defective reverse transcriptase inhibitors on the activity of n348i, a connection subdomain drug resistant HIV-1 reverse transcriptase mutant. *Cell. Mol. Biol.* 2012, **58** (1): 187-195.